Electron acoustic solitary waves with kappa-distributed electrons

To cite this article: S Devanandhan *et al* 2011 *Phys. Scr.* **84** 025507

Phys. Scr. **84** (2011) 025507 (6pp) doi:10.1088/0031-8949/84/02/025507

Electron acoustic solitary waves with kappa-distributed electrons

S Devanandhan[1], S V Singh[1,2] and G S Lakhina[1]

[1] Indian Institute of Geomagnetism, New Panvel (West), Navi Mumbai, India
[2] School of Physics, University of Kwazulu-Natal, Durban, South Africa

E-mail: satyavir@iigs.iigm.res.in

Received 17 February 2011
Accepted for publication 8 July 2011
Published 3 August 2011
Online at stacks.iop.org/PhysScr/84/025507

Abstract
Electron acoustic solitary waves are studied in a three-component, unmagnetized plasma composed of hot electrons, fluid cold electrons and ions having finite temperatures. Hot electrons are assumed to have kappa distribution. The Sagdeev pseudo-potential technique is used to study the arbitrary amplitude electron-acoustic solitary waves. It is found that inclusion of cold electron temperature shrinks the existence regime of the solitons, and soliton electric field amplitude decreases with an increase in cold electron temperature. A decrease in spectral index, κ, i.e. an increase in the superthermal component of hot electrons, leads to a decrease in soliton electric field amplitude as well as the soliton velocity range. The soliton solutions do not exist beyond $T_c/T_h > 0.13$ for $\kappa = 3.0$ and Mach number $M = 0.9$ for the dayside auroral region parameters.

PACS numbers: 52.35.g, 52.35.Fp, 52.35.Sb, 94.05.Fg

1. Introduction

Electrostatic solitary waves (ESWs) have been observed in various regions of the Earth's magnetosphere such as the magnetosheath, plasma sheet boundary layer, magnetotail, bow shock, magnetopause, auroral field lines, cusp and high-latitude polar magnetosphere [1–10]. These ESWs can be bipolar or tripolar pulses in the electric field component parallel to the background magnetic field. The amplitude of these solitary structures varies from a few $\mu\mathrm{V\,m^{-1}}$ in the plasma sheet boundary layer to $2.5\,\mathrm{V\,m^{-1}}$ in the auroral acceleration region [5].

Dysthe *et al* [11] studied the propagation of ESWs in a weakly magnetized plasma. They studied the nonlinear interaction of obliquely propagating Langmuir waves and low-frequency perturbations (ion-cyclotron or ion-sound waves). They also studied the modulational instability and the formation of envelope solitons and filamentation instabilities of the Langmuir waves. Later on, Christiansen *et al* [12] studied the filamentary collapse in electron-beam plasmas. It was shown that large-amplitude, beam-driven instabilities in obliquely propagating electron plasma and electron-cyclotron modes collapse into thin magnetic field aligned filaments. Giles [13] explained the results of Christiansen *et al* [12] through the coupling of upper hybrid waves and ion-cyclotron waves. Theoretical and experimental results have shown that filamentary collapse can occur in unmagnetized and magnetized plasmas [11–15]. Spatial collapse of Langmuir waves driven by an electron beam streaming into the solar wind upstream of Jupiter's bow shock has been observed by the Voyager spacecraft [16]. Langmuir wave collapse is believed to be important in ionosphere heating experiments by high-frequency waves [17–19].

Various theoretical studies have been carried out on electron-acoustic solitons. Duboluoz *et al* [20, 21] studied electron-acoustic solitons in an unmagnetized and magnetized two-electron-component and motionless ion plasma. They could explain the negative polarity electrostatic solitary potential structures observed by the Viking satellite in the dayside auroral zone. Positive polarity soliton structures have been studied in the auroral plasma by the FAST and POLAR spacecraft [22, 23]. Singh *et al* [24] studied electron-acoustic solitons in four-component plasmas and applied their results to Viking satellite observations in the dayside auroral zone. Mamun *et al* [25] studied obliquely propagating electron-acoustic solitons in magnetized plasma. Singh and Lakhina [26] examined the electron-acoustic solitons in unmagnetized plasmas with non-thermal distribution of electrons. A parametric study of high-frequency electrostatic oscillations in a three-component magnetized plasma has been conducted by Moolla *et al* [27]. Recently, compressive electron-acoustic solitons were studied by Verheest [28] without the electron-beam component. It was pointed out that positive potential structures can be obtained provided the hot electron inertia is retained in the analysis. Kakad *et al* [29] studied electron-acoustic solitons in a four-component unmagnetized plasma composed of cold background electrons, a cold electron beam, and cold and hot ions having Boltzmann distributions. The coexistence of rarefactive and compressive electron-acoustic solitary modes was predicted for specific plasma parameters. Ghosh *et al* [30] studied electron-acoustic solitary waves in a magnetized plasma consisting of warm electrons, a warm electron beam and two types of hot ions, and found that the characteristics and the existence domain of the positive potential electron-acoustic solitons are controlled by the ion temperature and concentration. Lakhina *et al* [31–33] studied ion and electron-acoustic solitary waves in three- and four-component plasmas and applied their results to the plasma sheet boundary layer and the magnetosheath plasma.

Most of the above studies on solitary waves are based on models using the Boltzmann distribution function for electrons/ions. But in space plasmas, a population of superthermal electrons where the particle distributions may deviate from the Maxwellian can exist [34–40]. These superthermal particles are described well by the kappa distributions, which involve the Maxwellian core and a high-energy tail component of the power-law form. The use of the kappa-distribution function was first introduced by Vasyliunas [41] to fit OGO 1 and OGO 2 solar wind data. This is an empirical fit to the observed particle distributions. Since then, it has been widely adopted by various researchers [42–49] to examine the effect of superthermal distributions on linear and nonlinear structures in ion- and dust-acoustic regimes.

Recently, Younsi and Tribeche [50] and Sahu [51] studied arbitrary amplitude electron-acoustic solitary waves in three-component unmagnetized plasmas with cold fluid electrons, hot superthermal (kappa-distributed) electrons and stationary ions. They found that the superthermal effects make the electron-acoustic structures more spiky. They have neglected the effect of cold electron temperature.

In this paper, their work is extended to include the thermal effects of cold electrons and ions by including the adiabatic equations of state. Also, ions are assumed to be mobile. In section 2, the theoretical model is discussed, then the numerical results are presented in section 3 and discussed in section 4.

2. Theoretical model

We consider a three-component, homogeneous, unmagnetized plasma comprising hot electrons, cold electrons and ions. The hot electrons are assumed to be following the kappa-distribution function given by [41]

$$f_{0\mathrm{h}}(v) = \frac{N_{0\mathrm{h}}}{\pi^{3/2}\theta^3}\frac{\Gamma(\kappa)}{\sqrt{\kappa}\,\Gamma(\kappa-1/2)}\left(1+\frac{v^2}{\kappa\theta^2}\right)^{-(\kappa+1)}, \qquad (1)$$

where $N_{0\mathrm{h}}$ is the hot electron density, κ is a parameter representing the spectral index of the distribution, $\Gamma(\kappa)$ is the gamma function and θ is a modified thermal speed given by

$$\theta^2 = \left(2-\frac{3}{\kappa}\right)\frac{k_\mathrm{B}T_\mathrm{h}}{m_\mathrm{e}}$$

with the spectral index $\kappa > 3/2$. Here T_h and m_e represent the hot electron temperature and electron mass, respectively. When $\kappa \to \infty$, the kappa-distribution function given by (1) reduces to a Maxwellian distribution. Replacing $\frac{v^2}{\theta^2}$ by $\frac{v^2}{\theta^2} - \frac{2e\phi}{m\theta^2}$, where ϕ is the electrostatic potential and e is the electrostatic charge, one can obtain the distribution function for electrons in the presence of non-zero potential and integration of this gives the following number density for electrons:

$$n_\mathrm{h} = n_{0\mathrm{h}}\left(1-\frac{\phi}{(\kappa-3/2)}\right)^{-(\kappa-1/2)}. \qquad (2)$$

The cold electrons and ions are assumed to be mobile and are governed by the following fluid equations:
the continuity equation

$$\frac{\partial n_j}{\partial t} + \frac{\partial}{\partial x}(n_j v_j) = 0, \qquad (3)$$

the momentum equation

$$\frac{\partial v_j}{\partial t} + v_j\frac{\partial v_j}{\partial x} + \frac{1}{\mu_j n_j}\frac{\partial P_j}{\partial x} - \frac{Z_j}{\mu_j}\frac{\partial\phi}{\partial x} = 0, \qquad (4)$$

the equation of state

$$\frac{\partial P_j}{\partial t} + v_j\frac{\partial P_j}{\partial x} + 3P_j\frac{\partial v_j}{\partial x} = 0 \qquad (5)$$

and the Poisson equation

$$\frac{\partial^2\phi}{\partial x^2} = n_\mathrm{h} + n_\mathrm{c} - n_\mathrm{i}. \qquad (6)$$

Here n_j, v_j and P_j are the density, fluid velocity and pressure of the jth species, where $j = \mathrm{c, i}$ represent cold electrons and ions, respectively, $Z_j = \pm 1$ for electrons and ions, respectively, and $\mu_j = m_j/m_\mathrm{e}$. Equations (2)–(6) are a normalized set of equations. We have normalized densities by the total equilibrium electron (ion) density $N_0 = N_{0\mathrm{h}} + N_{0\mathrm{c}} = N_{0\mathrm{i}}$, velocities by the thermal velocity of hot electrons $v_\mathrm{th} = \sqrt{T_\mathrm{h}/m_\mathrm{e}}$, lengths by the effective hot electron Debye length $\lambda_\mathrm{dh} = \sqrt{T_\mathrm{h}/4\pi N_0 e^2}$, temperature by the hot electron temperature T_h, time by the inverse of the electron plasma frequency $\omega_\mathrm{pe}^{-1} = \sqrt{m_\mathrm{e}/4\pi N_0 e^2}$, the potential by T_h/e and the thermal pressure by $N_0 T_\mathrm{h}$. The linear dispersion relation can be obtained from the set of equations (2)–(6) and can be written in unnormalized form as

$$1 + \frac{1}{k^2\lambda_\mathrm{dh}^2}\left(\frac{\kappa-1/2}{\kappa-3/2}\right) - \frac{\omega_\mathrm{pc}^2}{(\omega^2-3k^2v_\mathrm{tc}^2)} - \frac{\omega_\mathrm{pi}^2}{(\omega^2-3k^2v_\mathrm{ti}^2)} = 0, \qquad (7)$$

where $\omega_{\mathrm{p}j} = \sqrt{4\pi N_{0j}e^2/m_j}$ and $v_{\mathrm{t}j} = \sqrt{T_j/m_j}$ are the plasma frequency and thermal speed of the jth species and N_{0j}, T_j and m_j are the equilibrium density, temperature and mass of the jth species, respectively. The linear dispersion relation (7) can be written as

$$\omega^4 - \omega^2\left[3k^2v_\mathrm{tc}^2 + 3k^2v_\mathrm{ti}^2 + \frac{\omega_\mathrm{pc}^2+\omega_\mathrm{pi}^2}{a}\right] + 9k^4v_\mathrm{tc}^2v_\mathrm{ti}^2 + \frac{3k^2v_\mathrm{tc}^2\omega_\mathrm{pi}^2 + 3k^2v_\mathrm{ti}^2\omega_\mathrm{pc}^2}{a} = 0, \qquad (8)$$

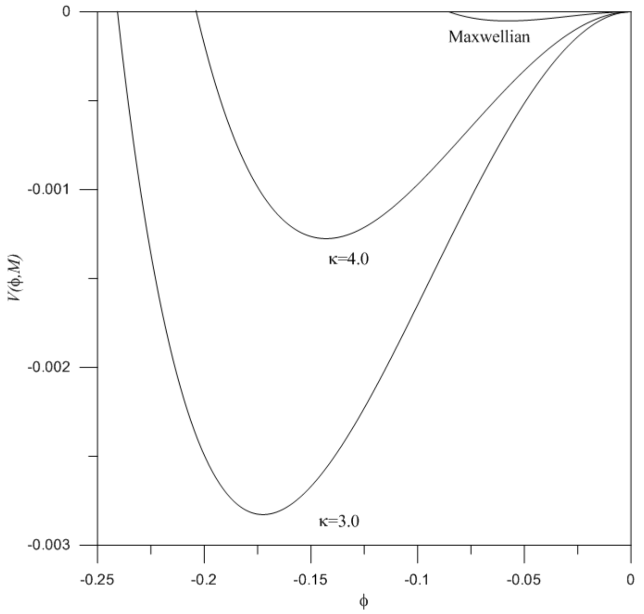

Figure 1. Variation of the Sagdeev potential $V(\phi, M)$ with ϕ for κ=3, 4 and $\kappa = \infty$ (Maxwellian) for $n_{0c} = 0.4$, $n_{0h} = 0.6$, $\sigma_c = T_c/T_h = 0.01 = T_i/T_h = \sigma_i$ and Mach number $M = 0.9$.

where

$$a = 1 + \frac{1}{k^2\lambda_{dh}^2}\left(\frac{\kappa - 1/2}{\kappa - 3/2}\right).$$

The dispersion relation (8) is quadratic in ω^2 and can be simplified to give two linear modes of the plasma, i.e. the electron-acoustic mode

$$\omega^2 = k^2 v_{th}^2\left[\frac{\left((\kappa-3/2)/(\kappa-1/2)\right)\left(N_{0c}/N_{0h}\right)}{1+\left((\kappa-3/2)/(\kappa-1/2)\right)k^2\lambda_{dh}^2} + \frac{3T_c}{T_h}\right], \tag{9}$$

which is the same as that of Hellberg *et al* [52] and can be further simplified in the limit

$$\left(\frac{\kappa-3/2}{\kappa-1/2}\right)k^2\lambda_{dh}^2 \ll 1$$

to give

$$\omega^2 = k^2 v_{th}^2\left[\frac{3T_c}{T_h} + \frac{N_{0c}}{N_{0h}}\frac{\kappa-3/2}{\kappa-1/2}\right]. \tag{10}$$

It is clear from equation (10) that the linear dispersion relation from the electron-acoustic mode is modified due to the presence of superthermal electrons. For $\kappa \to \infty$, equation (10) gives the usual expression for the electron-acoustic mode in Maxwellian plasmas. The second mode is the ion-acoustic mode given by

$$\omega = kc_s\left[\frac{T_i}{T_c} + \frac{\left(N_{0i}/N_{0h}\right)\left((\kappa-3/2)/(\kappa-1/2)\right)}{(3T_c/T_h) + \left(N_{0c}/N_{0h}\right)\left((\kappa-3/2)/(\kappa-1/2)\right)}\right]^{1/2}, \tag{11}$$

where $c_s = (3T_c/m_i)^{1/2}$ is the ion-acoustic speed defined with respect to cold electron temperature. In the case of $N_c = 0$ and $\kappa \to \infty$, the usual ion-acoustic mode in pure electron–ion plasmas is recovered. In this paper, we will focus on electron-acoustic modes. To study the properties of stationary, arbitrary amplitude electron-acoustic solitons, we transform the above set of equations (2)–(6) to a stationary frame moving with velocity V, the phase velocity of the wave, i.e. $\xi = (x - Mt)$, where $M = V/v_{th}$ is the Mach number. Further, solving for the perturbed densities of electrons and ions and substituting these expressions into the Poisson equation, and assuming appropriate boundary conditions for the localized disturbances along with the conditions that potential $\phi = 0$, and $d\phi/d\xi = 0$ at $\xi \to \pm\infty$, we obtain the following energy integral:

$$\frac{1}{2}\left(\frac{d\phi}{d\xi}\right)^2 + V(\phi, M) = 0, \tag{12}$$

where

$$\begin{aligned}
V(\phi, M) = {} & n_{0h}\left[1 - \left(1 - \frac{\phi}{\kappa - 3/2}\right)^{-(\kappa-3/2)}\right] \\
& + n_{0c}\left[M^2 - \frac{M}{\sqrt{2}}\left\{M^2 + 3\sigma_c + 2\phi\right.\right. \\
& \left.\left. + \sqrt{(M^2+3\sigma_c+2\phi)^2 - 12\sigma_c M^2}\right\}^{1/2}\right] \\
& + n_{0c}\sigma_c\left[1 - 2\sqrt{2}M^3\left\{M^2 + 3\sigma_c + 2\phi\right.\right. \\
& \left.\left. + \sqrt{(M^2+3\sigma_c+2\phi)^2 - 12\sigma_c M^2}\right\}^{-3/2}\right] \\
& + \mu_i\left[M^2 - \frac{M}{\sqrt{2}}\left\{M^2 + \frac{3\sigma_i}{\mu_i} - \frac{2\phi}{\mu_i}\right.\right. \\
& \left.\left. + \sqrt{\left(M^2 + \frac{3\sigma_i}{\mu_i} - \frac{2\phi}{\mu_i}\right)^2 - \frac{12\sigma_i M^2}{\mu_i}}\right\}^{1/2}\right] \\
& + \sigma_i\left[1 - 2\sqrt{2}M^3\left\{M^2 + \frac{3\sigma_i}{\mu_i} - \frac{2\phi}{\mu_i}\right.\right. \\
& \left.\left. + \sqrt{\left(M^2 + \frac{3\sigma_i}{\mu_i} - \frac{2\phi}{\mu_i}\right)^2 - \frac{12\sigma_i M^2}{\mu_i}}\right\}^{-3/2}\right]
\end{aligned} \tag{13}$$

is the pseudo-potential known as the Sagdeev potential and $\sigma_c = T_c/T_h$, $\sigma_i = T_i/T_h$, $n_{0c} = N_{0c}/N_0$ and $n_{0h} = N_{0h}/N_0$. Equation (12) yields solitary wave solutions when the Sagdeev potential $V(\phi, M)$ satisfies the following conditions: $V(\phi, M) = 0$, $dV(\phi, M)/d\phi = 0$ and $d^2V(\phi, M)/d\phi^2 < 0$ at $\phi = 0$; $V(\phi, M) = 0$ at $\phi = \phi_m$ and $V(\phi, M) < 0$ when $0 < |\phi| < |\phi_m|$, where ϕ_m is the maximum potential. From equation (13), it is seen that $V(\phi, M)$ and its first derivative with respect to ϕ vanish at $\phi = 0$. The condition $d^2V(\phi, M)/d\phi^2 < 0$ at $\phi = 0$ is satisfied provided $M > M_0$, where M_0 is the critical Mach number and satisfies the following equation:

$$\frac{n_{0c}}{\left(M_0^2 - 3\sigma_c\right)} + \frac{1}{\mu_i\left(M_0^2 - (3\sigma_i/\mu_i)\right)} = n_{0h}\left(\frac{\kappa-1/2}{\kappa-3/2}\right), \tag{14}$$

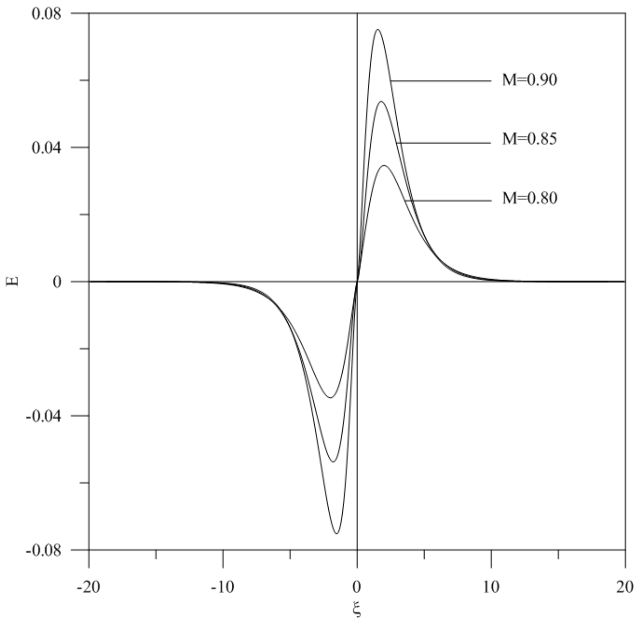

Figure 2. Variation of the normalized electric field amplitude E with ξ for Mach numbers $M = 0.8$, 0.85 and 0.9 for $\kappa = 3$. The other parameters are the same as those in figure 1.

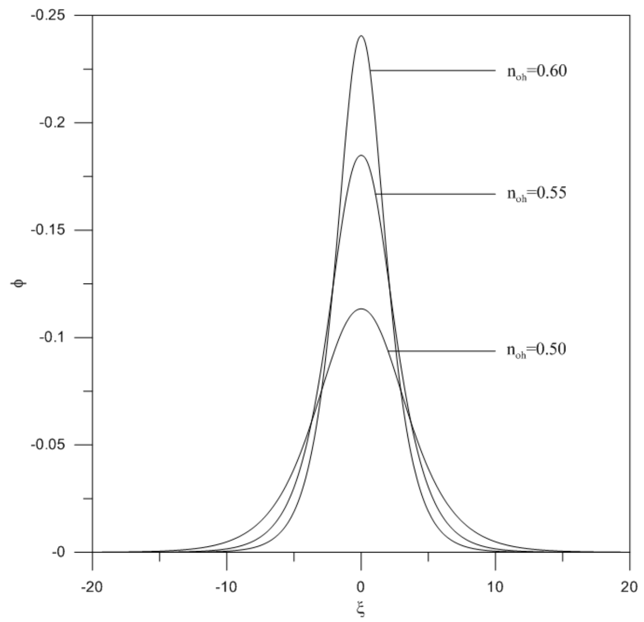

Figure 3. Variation of the normalized electric potential ϕ with ξ for $n_{0h} = 0.5$, 0.55 and 0.6 as shown on the curves and for $\kappa = 3$. The other fixed parameters are the same as those in figure 1.

and is approximately given by

$$M_0 \approx \sqrt{\frac{n_{0c}}{n_{0h}}\left(\frac{\kappa - 3/2}{\kappa - 1/2}\right) + 3\sigma_c}, \qquad (15)$$

where the contribution from ions has been neglected. However, in general, equation (14) yields four roots but all the roots will not be physical. For numerical computations, only the real positive roots of the critical Mach numbers will be considered.

3. Numerical results

Figure 1 shows the variation of the Sagdeev potential $V(\phi, M)$ with normalized potential ϕ for different values of the spectral index $\kappa = 3, 4$ and $\kappa = \infty$ (Maxwellian) as shown in the curves. The typical chosen values of the normalized parameters are: cold electron density $n_{0c} = 0.4$, hot electron density $n_{0h} = 0.6$, cold electron to hot electron temperature ratio $\sigma_c = T_c/T_h = 0.01 = T_i/T_h$ ($= \sigma_i$, the ion to hot electron temperature ratio) and Mach number $M = 0.9$. It can be seen from the figure that the amplitude of the electron-acoustic solitons decreases with an increase in the spectral index κ. For the above parameters, the soliton solution does not exist beyond $T_c/T_h > 0.13$ for $\kappa = 3$. It must be pointed out that depending on the parameters there will be different limits on the T_c/T_h value beyond which a soliton solution may not exist.

Figure 2 shows the variation of the normalized electric field amplitude, E, with ξ for the Mach numbers $M = 0.8$, 0.85 and 0.9 for $\kappa = 3$. The other parameters are the same as those for figure 1. It is clear from the figures that the electric field amplitude of the bipolar structures increases with an increase in Mach number. On the other hand, it is observed that soliton width decreases with an increase in Mach number.

Table 1. Properties of electron-acoustic solitons such as the soliton velocity (V), electric field (E), soliton width (W) and pulse duration (τ) for various values of the spectral index κ for $n_{0c} = 0.40$, $n_{0h} = 0.60$ and $\sigma_c = T_c/T_h = 0.01 = T_i/T_h = \sigma_i$. The dayside auroral region parameters [21], namely hot electron temperature, $T_h = 250$ eV, cold electron temperature, $T_c = 2.5$ eV $= T_i$ (ion temperature), and total electron density, $N_0 = 2.7\,\mathrm{cm}^{-3}$, are used for the numerical estimates of V, E, W and τ.

κ	V (km s^{-1})	E (mV m^{-1})	W (m)	$\tau = W/V$ (μs)
2.0	3336−4733	0.06−230	2383−193	714−41
3.0	4362–6552	0.18−411	2719−245	623−37.4
4.0	4733−7184	0.21−477	2792−265	590−36.9
5.0	4932−7510	0.35−512	2857−275	580−36.7

Figure 3 shows the profiles of the normalized electric potential, ϕ, with ξ for various values of the hot electron density, $n_{0h} = 0.5$, 0.55 and 0.6 as shown in the curves and for $\kappa = 3$. The rest of the parameters are the same as those for figure 1. The amplitude of ϕ increases with an increase in hot electron density but the soliton width decreases.

In tables 1 and 2, we give the unnormalized values of the soliton velocity (V), electric field (E), soliton width (W) and pulse duration (τ) for various values of spectral index κ and $T_c/T_h = T_i/T_h$, respectively. For illustrative purposes, we have used dayside auroral region parameters [21]. It is clear from table 1 that the soliton velocity, electric field amplitude and width tend to increase with κ, but pulse duration seems to decrease. Also, the range of soliton velocities tends to increase with κ. From table 2, it is interesting to note that the maximum electric field amplitude of the soliton for the case of $T_c/T_h = 0$ is about $3\,\mathrm{V\,m^{-1}}$, which is on the higher side for the auroral region. However, for finite values of T_c/T_h, e.g. $T_c/T_h = 0.01$, the maximum electric field amplitude is about $400\,\mathrm{mV\,m^{-1}}$, and it subsequently decreases with further increase in T_c/T_h value.

Table 2. Variation of the soliton velocity (V), electric field (E), soliton width (W) and pulse duration (τ) of the electron-acoustic solitons for various values of $\sigma_c = T_c/T_h$ $(= T_i/T_h)$ for $n_{0c} = 0.40$, $n_{0h} = 0.60$ and $\kappa = 3.0$. The dayside auroral region parameters [21], namely hot electron temperature, $T_h = 250$ eV, cold electron temperature, $T_c = 2.5$ eV $= T_i$ (ion temperature), and total electron density, $N_0 = 2.7$ cm^{-3}, are used for the numerical estimates of V, E, W and τ.

$T_c/T_h = T_i/T_h$	V (km s^{-1})	E (mV m^{-1})	W (m)	$\tau = W/V$ (μs)
0.00	4203–14028	0.086–3067	3176–201	756–14.3
0.01	4362–6552	0.18–411	2719–245	623–37.4
0.02	4514–6186	0.25–276	2230–277	494–44.7
0.04	4806–6033	0.46–173	1954–285	407–47.3
0.05	4945–6046	0.56–146	1735–288	351–47.6

4. Discussion and conclusions

Electron-acoustic solitons are studied in three-component, unmagnetized plasma having kappa-distributed hot electrons, cold fluid electrons and fluid ions. Thermal effects of cold fluid electrons are taken into account, which were neglected by Younsi and Tribeche [50]. For computational purposes, we have used the plasma parameters associated with the electrostatic solitary structures observed in the dayside auroral region of the Earth's magnetosphere by the Viking satellite [21]. It is observed that the decrease in the spectral index κ (i.e. more superthermal electrons) leads to a reduction in the range of soliton velocity (V), electric field (E) and soliton width (W) but an increase in the soliton pulse duration (τ), as is seen from table 1.

Table 2 clearly shows that the inclusion of cold electron temperature significantly reduces the regime for the existence of the solitons and their electric field decreases with an increase in cold electron temperature. For example, for $T_c/T_h = 0$ the maximum electric field amplitude is about 3 V m^{-1} (see column 3, row 1 of table 2), whereas for the nominal value of $T_c/T_h = 0.05$, it drastically reduces to about $\sim$140 mV m^{-1} (see the last row, column 3 of table 2). Similarly, there is more than 50% reduction in the maximum soliton velocity, width and pulse duration for the case of $T_c/T_h = 0.05$ as compared with the $T_c/T_h = 0.0$ case (see the first and last rows of table 2, columns 2, 4 and 5). Further, the ranges of soliton velocity (V), electric field (E), soliton width (W) and pulse duration (τ) decrease as the cold electron temperature is increased.

To summarize, the inclusion of cold electron temperature shrinks the existence regime of the solitons and at the same time reduces the soliton electric field amplitude. The results obtained here may be helpful in explaining the characteristics of the solitary structures observed by Viking. We must point out that the auroral plasma where Viking made the measurements is strongly magnetized. However, parallel propagating electron-acoustic waves are not affected by the presence of the background magnetic field [21]. Therefore, our theory should remain valid for solitary structures propagating parallel to the magnetic field. At present, we are studying the obliquely propagating electron-acoustic waves in a magnetized plasma system, and the results will be reported elsewhere.

Acknowledgment

GSL acknowledges support from the Indian National Science Academy (New Delhi, India) under the Senior Scientist scheme.

References

[1] Matsumoto H, Kojima H, Miyatake T, Omura Y, Okada M, Nagano I and Tsutsui M 1994 *Geophys. Res. Lett.* **21** 2915–8
[2] Kojima H, Matsumoto H, Chikuba S, Horiyama S, Ashour-Abdalla M and Anderson R R 1997 *J. Geophys. Res.* **102** 14439–55
[3] Mozer F S, Ergun R, Temerin M, Cattell C, Dombeck J and Wygant J 1997 *Phys. Rev. Lett.* **79** 1281–4
[4] Bostrom R, Gustafsson G, Holback B, Holmgren G, Koskinen H and Kintner P 1988 *Phys. Rev. Lett.* **61** 82–5
[5] Ergun R E *et al* 1998 *Geophys. Res. Lett.* **25** 2041–4
[6] Bale S D, Kellogg P J, Larsen D E, Lin R P, Goetz K and Lepping R P 1998 *Geophys. Res. Lett.* **25** 2929–32
[7] Cattell C, Dombeck J, Wygant J R, Hudson M K, Mozer F S, Temerin M A, Peterson W K, Kletzing C A, Russell C T and Pfaff R F 1999 *Geophys. Res. Lett.* **26** 425–8
[8] Bounds S R, Pfaff R F, Knowlton S F, Mozer F S, Temerin M A and Kletzing C A 1999 *J. Geophys. Res.* **104** 28709–17
[9] Pickett J S *et al* 2004 *Nonlinear Proc. Geophys.* **11** 183–96
[10] Pickett J S *et al* 2005 *Nonlinear Proc. Geophys.* **12** 181–93
[11] Dysthe K B, Miolhus E, Pecseli H L and Stenflo L 1978 *Plasma Phys.* **20** 1087–99
[12] Christiansen P J, Jain V K and Stenflo L 1981 *Phys. Rev. Lett.* **46** 1333–7
[13] Giles M J 1981 *Phys. Rev. Lett.* **47** 1606–8
[14] Thornhill S G and ter Haar D 1978 *Phys. Rep.* **43** 43–99
[15] Rudakov L I and Tsytovich V N 1978 *Phys. Rep.* **40** 1–73
[16] Gurnett D A, Maggs J E, Gallagher D L, Kurth W S and Scarf F L 1981 *J. Geophys. Res.* **86** 8833–41
[17] Sulzer M P and Fejer J A 1994 *J. Geophys. Res.* **99** 15035–50
[18] DuBois D F, Russell D and Rose H A 1995 *Phys. Plasmas* **2** 76–96
[19] Wang J G, Newman D L and Goldman M V 1997 *J. Atmos. Solar-Terres. Phys.* **59** 2461–74
[20] Dubouloz N, Pottelette R, Malingre M, Holmgren G and Lindqvist P A 1991 *J. Geophys. Res.* **96** 3565–79
[21] Dubouloz N, Trueman R A, Pottelette R and Malingre M 1993 *J. Geophys. Res.* **98** 17415–22
[22] Berthomier M, Pottelette R, Malingre M and Khotyaintsev Y 2000 *Phys. Plasmas* **7** 2987–94
[23] Berthomier M, Pottelette R, Muschietti L, Roth I and Carlson C W 2003 *Geophys. Res. Lett.* **30** 2148
[24] Singh S V, Reddy R V and Lakhina G S 2001 *Adv. Space. Res.* **28** 1643–8
[25] Mamun A A, Shukla P K and Stenflo L 2002 *Phys. Plasmas* **9** 1474–7
[26] Singh S V and Lakhina G S 2004 *Nonlinear Proc. Geophys.* **11** 275–9
[27] Moolla S, Bharuthram R, Singh S V, Lakhina G S and Reddy R V 2007 *J. Geophy. Res.* **112** A07214
[28] Verheest F 2009 *Phys. Plasmas* **16** 013704
[29] Kakad A P, Singh S V, Reddy R V, Lakhina G S, Tagare S G and Verheest F 2007 *Phys. Plasmas* **14** 052305
[30] Ghosh S S, Pickett J S, Lakhina G S, Winningham J D, Lavraud B and Décréau P M E 2008 *J. Geophys. Res.* **113** A06218
[31] Lakhina G S, Kakad A P, Singh S V and Verheest F 2008 *Phys. Plasmas* **15** 062903
[32] Lakhina G S, Singh S V, Kakad A P, Verheest F and Bharuthram R 2008 *Nonlinear Proc. Geophys.* **15** 903–13

[33] Lakhina G S, Singh S V, Kakad A P, Goldstein M L, Vinas A F and Pickett J S 2009 *J. Geophys. Res.* **114** A09212
[34] Scudder J D, Sittler E C and Bridge H S 1981 *J. Geophys. Res.* **86** 8157–79
[35] Sarris E T, Krimigis S M, Lui A T Y, Ackerson K L, Frank L A and Williams D J 1981 *Geophys. Res. Lett.* **8** 349–52
[36] Marsch E, Muhlhauser K H, Schwenn R, Rosenbauer H, Pillip W and Neubauer F M 1982 *J. Geophys. Res.* **87** 52–72
[37] Christon S P, Williams D J, Mitchell D G, Frank L A and Huang C Y 1989 *J. Geophys. Res.* **94** 13409–24
[38] Christon S P, Mitchell D G, Williams D J, Frank L A, Huang C Y and Eastman T E 1988 *J. Geophys. Res.* **93** 2562–72
[39] Pisarenko N F, Budnik E Yu, Ermolaev Yu I, Kirpichev I P, Lutsenko V N, Morozova E I and Antonova E E 2002 *J. Atmos. Solar-Terres. Phys.* **64** 573–83
[40] Andersson L, Newman D L, Ergun R E, Goldman M V, Carlson C W and McFadden J P 2008 *Phys. Plasmas* **15** 072901
[41] Vasyliunas V M 1968 *J. Geophys. Res.* **73** 2839–84
[42] Abbasi H and Hakimi Pajouh H 2007 *Phys. Plasmas* **14** 012307
[43] Baluku T K and Hellberg M A 2008 *Phys. Plasmas* **15** 123705
[44] Antonova E E and Ermakova N O 2008 *Adv. Space Res.* **42** 987–91
[45] Hau L N and Fu W Z 2007 *Phys. Plasmas* **14** 110702
[46] Hau L N, Fu W Z and Chuang S H 2009 *Phys. Plasmas* **16** 094702
[47] Hellberg M A, Mace R L, Baluku T K, Kourakis I and Saini N S 2009 *Phys. Plasmas* **16** 094701
[48] Gill T S, Bains A S and Bedi C 2010 *Phys. Plasmas* **17** 013701
[49] Jung Y D and Hong W P 2011 *Phys. Plasmas* **18** 024502
[50] Younsi S and Tribeche M 2010 *Astrophys. Space Sci.* **330** 295–300
[51] Sahu B 2010 *Phys. Plasmas* **17** 122305
[52] Hellberg M A, Mace R L, Armstrong R J and Karlstad G 2000 *J. Plasma Phys.* **64** 433–43